

Young Stellar Objects and Herbig–Haro Objects*

W. J. Zealey

Department of Physics, University of Wollongong,
Box 1144, Wollongong, N.S.W. 2500, Australia.

Abstract

Our current understanding of Herbig–Haro objects and their relationship with young stellar outflows is reviewed. The role of multi-waveband observations in the visible, infrared and radio in the study of outflows is discussed with examples drawn from the HH1, HH24 and HH54 outflow complexes. The current theories are briefly considered in the light of spectroscopic and morphological data. It is concluded that although the general mechanism of outflows is understood, the details of the outflowing material's origin and the collimation mechanism remain largely unanswered.

1. Introduction

Over the past decade it has become widely accepted that supersonic mass loss plays a major role in the early evolution of most young stellar objects (YSOs). These outflows often have Mach numbers in excess of 10 and mass loss rates of between $10^{-8} M_{\odot} \text{ yr}^{-1}$ and $10^{-6} M_{\odot} \text{ yr}^{-1}$. Outflows in nearby molecular cloud complexes, where they can be studied at high spatial resolution with high sensitivity, provide excellent laboratories for understanding the outflow phase of star formation.

The detailed character of the interaction between the outflows and the interstellar medium (ISM) has been reviewed by Schwartz (1983, 1985), Mundt (1988) and most recently by Reipurth (1991). The signatures for such outflows and their driving sources include visible and infrared emission nebulosity, with characteristics of shock excitation; infrared and visible reflection nebulae; broad asymmetric molecular emission lines and small, but extended regions of radio emission.

A distinction is often made between two classes of outflow:

Molecular outflows are highly obscured and associated with high luminosity driving sources ($L > 1000L_0$) observable in the far infrared. In general no optical tracers are found in the flows.

Optical bipolar outflows are less obscured and have low luminosity driving sources observable in the visible and near infrared (T-Tauri/FU Orionis stars, $L < 500L_0$). They are usually associated with visible and near infrared emission

* Paper presented at the Workshop on Star Formation in Different Environments, held at the University of Sydney, 9–11 October 1991.

nebulosity (jets, Herbig–Haro objects). The mass loss rates inferred from CO emission observations are lower than those of ‘molecular outflows’.

The difference between the two may be an observational selection effect due to the increase in scale size associated with the visible features as the luminosity of the driving source increases (Rodriguez 1989). Recently Poetzel *et al.* (1989) have detected visible Herbig–Haro (HH) objects associated with Z CMa, which has a luminosity $L = 3500L_0$.

In this paper we concentrate on summarising some of the observational tools available for the study of the *optical bipolar outflows* and their associated HH objects and on illustrating their application using the HH24 and HH54 outflow complexes as examples.

2. Survey Methods

(2a) Photographic: Schwartz (1977) and Reipurth (1991)

On direct photographic, red survey plates (ESO/SERC/Palomar Surveys) the first indication of star formation often takes the form of small red HH nebulosities with extents of less than $1'$. These often occur in groups or alignments and are most easily seen in projection against dark clouds. Follow-up objective prism spectroscopy shows that many of these nebulae exhibit strong Balmer and [OI], [NII] and [SII] emission lines.

(2b) Infrared: Suters and Zealey (1991), McCutcheon *et al.* (1991), Evans and Lada (1991)

With the advent of almost complete far infrared surveys (e.g. IRAS), it is possible to use [12–25], [25–60] colour–colour diagrams to identify young stellar objects. Selected objects can then be studied at visible, infrared and millimetre wavelengths for indications of outflows. In at least one case (HH54) the whole of the 60 IRAS flux appears to be associated with the HH object itself and probably arises as a result of [OI] emission at 63 (Fig. 1).

3. Visible, Infrared and Radio Morphology

High resolution, narrow band CCD frames and prime focus photographic plates of outflow complexes clearly show some or all of the following features (Fig. 2):

- (i) A central source.
- (ii) A collimated jet.
- (iii) A transition region where the jet disappears.
- (iv) A working surface and associated HH complex.

(3a) The Central Source

Sources associated with molecular outflows cover a wide range of luminosities of over six orders of magnitude. In contrast, sources traditionally associated with visible jets and HH objects have bolometric luminosities of between 1 – $700L_0$ (Berrilli *et al.* 1989). These sources which include visible T-Tauri stars (Appenzeller 1988) and FU Orionis stars (Reipurth 1989) are therefore comparatively low luminosity objects. The stars where visible often show highly developed P Cygni emission profiles associated with mass outflow. The terminal velocities derived from such

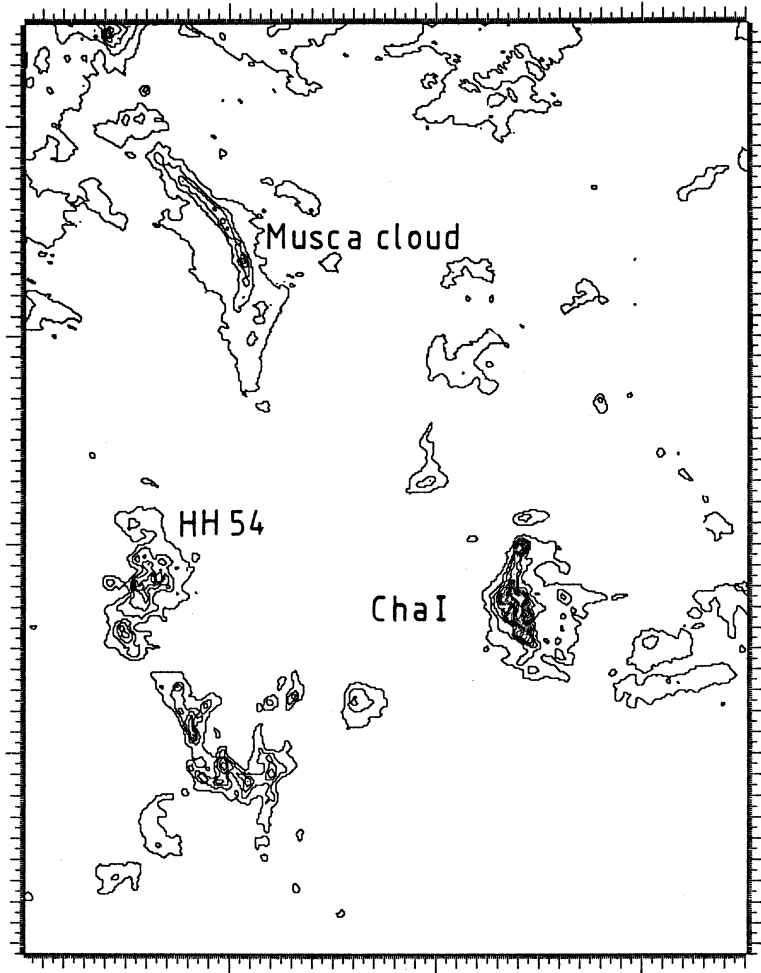


Fig. 1. An IRAS 100 flux map of the Chameleon complex, showing HH54 and Cha I.

profiles lie in the range $100\text{--}400\text{ km s}^{-1}$, similar to the radial velocities of the jets themselves, with associated mass loss rates of 10^{-9} to $10^{-7} M_{\odot} \text{ yr}^{-1}$.

In many sources, optical reflection nebulae, indicative of a circumstellar disk, may be detected near the source. In the case of sources like R Mon (Jones and Herbig 1982) this results in a highly visible biconical or cometary nebula, the axis of which is closely aligned with the jets.

In a number of complexes the central source is highly obscured and is visible only at infrared or radio wavelengths. The infrared source SSV63E in M78 provides a good example of the range of observations possible (Zealey *et al.* 1989, 1992). Near infrared images and photometry, coupled with IRAS data, show that SSSV63E suffers up to 50 magnitudes of visual extinction from a disk aligned closely to our line of sight (Fig. 3). Evidence for this disk is seen in the form of adjacent pairs of infrared and optical reflection nebulosities lying on either side of SSV63E (Fig. 4). A VLA radio continuum source, though associated with the outflow and disk structure, does not lie on the projected line of the jets.

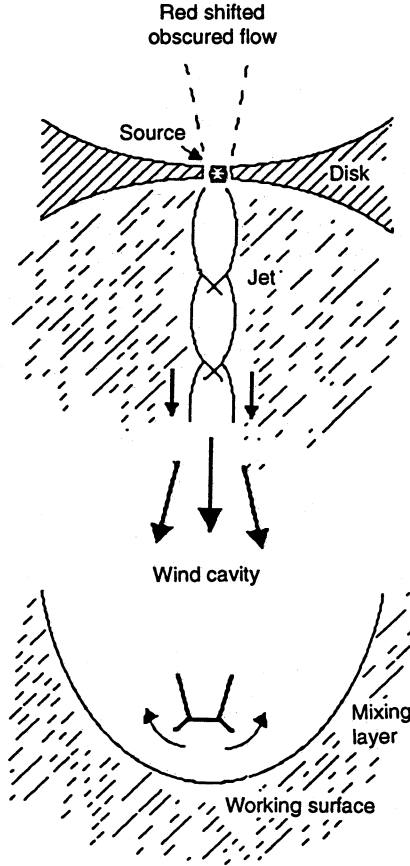


Fig. 2. A diagram of a typical outflow complex.

Infrared spectroscopy at $2\ \mu\text{m}$ of bright sources can be a powerful technique for identifying possible YSOs associated with outflows. The presence of Brackett γ and, as in the case of SSV63E, the first overtone bands of CO in emission [seen also in outflow sources SSV13, DGTau, AS353A and 1458C27 (McGregor *et al.* 1988; Carr 1989)] are indicative of excited atomic and molecular gas associated with a circumstellar disk, the outer layers of the stellar atmosphere or the outflow itself.

Imaging polarimetry in the visible and infrared provides additional evidence for disks (Aspin *et al.* 1992). Scarrott *et al.* (1987) interpreted the strong centro-symmetric pattern of polarisation vectors seen in the HH24 complex as evidence that SSV63E is the principal source illuminating the visible nebulosity.

(3b) The Jets

Morphology of jets: More than twenty optical jets associated with young stellar objects are known, the best example being HH34 (Mundt *et al.* 1987).

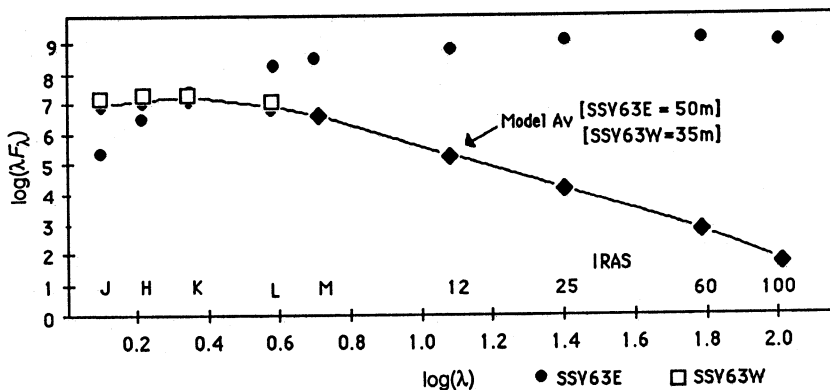


Fig. 3. Near infrared photometry of SSV63E (the driving source of HH24) and the reflection nebulosity SSV63W (Anglo Australian Telescope).

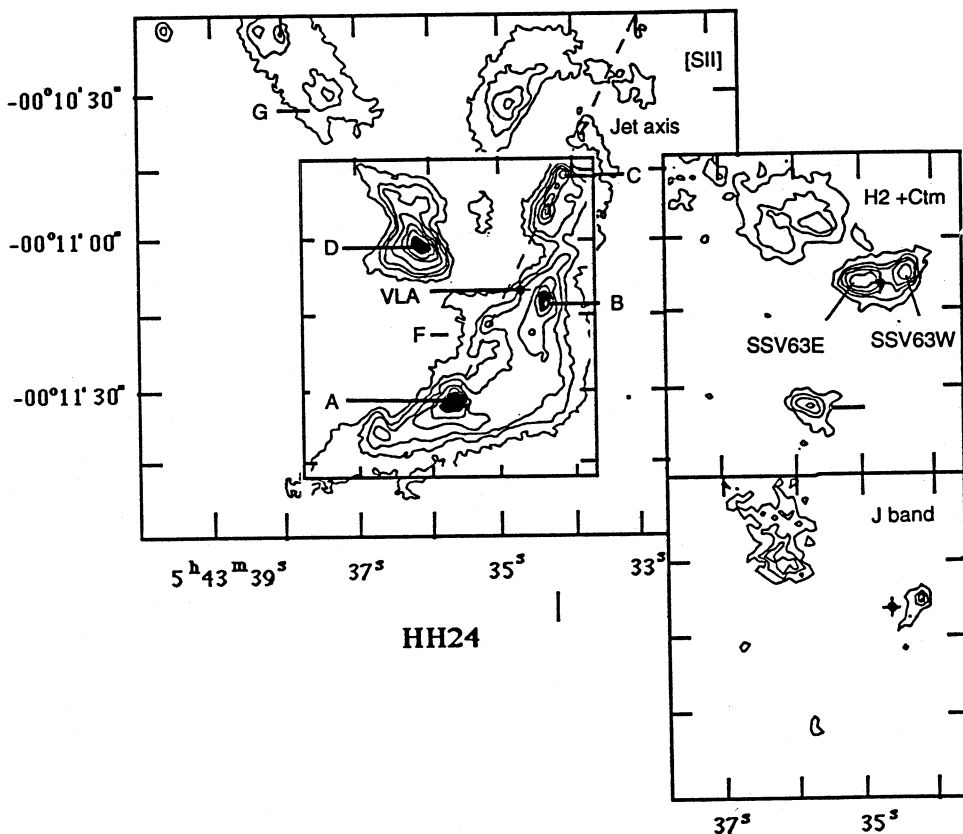


Fig. 4. Infrared and visible maps of the HH24 complex, showing the paired IR and visible sources interpreted as due to reflection from a disk (AAT and UKIRT). Herbig-Haro objects are lettered A to G.

Well collimated jets often consist of strings of roughly equidistant knots. These are usually aligned with bright cusps or extended clumps of emission nebulosity (HH objects) which are interpreted as the working surfaces of the jets. The jets typically have lengths between 0.01 and 1 pc and opening angles between 1° and 10° .

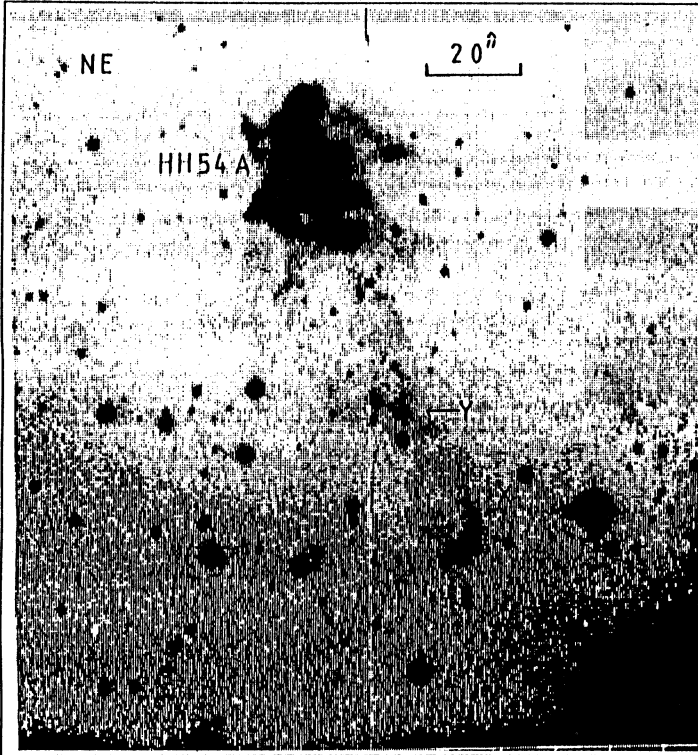


Fig. 5. A gunn r CCD frame of HH54 (Danish 1.5 m).

In a number of sources both red and blue velocity-shifted jets are observed. In such cases there are often obvious differences in both the morphology and spectra of the opposed jets due, in part, to the jets encountering different density conditions as they expand. Examples may be found in M78/HH24 and HH54 (Fig. 5). Few jets are perfectly straight. Many have 'wiggles' superimposed on them (HH30, HH7-11, HH46/47; see Lightfoot and Glencross 1986). Such behaviour has led several authors to consider precessing jet models of varying complexity.

Radio continuum emission has been observed not only from the central stars of outflow complexes, but also from the region of the jets. This emission is often found to be elongated along the flow axis, as observed in L1551 IRS5. The VLA source CrA IRS7 shows a particularly complex structure, featuring two bright compact sources and extended emission along the axis of the flow (Brown 1987). In some cases, but not all, the spectral index is indicative of a nonthermal process (Bieging *et al.* 1986).

Spectroscopy of jets: Long slit spectroscopy has proved a powerful method allowing observations to be made of velocity, velocity dispersion, electron density and excitation along the jets (Mundt *et al.* 1987; Cohen *et al.* 1987). The emission spectra of the knots in the jets strongly resemble those observed in recombination regions behind low velocity shocks.

The spectra of the knots is generally that of a low excitation gas heated by a comparatively slow shock $V_s = 50 \text{ km s}^{-1}$. With the exception of reflected light from the driving source, little optical continuum radiation is observed from the jets. The dominant emission is in the recombination lines of $H\alpha$ and forbidden emission lines ([SII], [OI] etc.). The ratio of the intensity of the [SII] lines at 671.6 and 673.1 nm indicates that jet electron densities are typically $400\text{--}2000 \text{ cm}^{-3}$. This leads to an estimate of jet densities in the region of $20\text{--}100 \text{ H atoms cm}^{-3}$. In many cases the density decreases away from the source, as expected for a constant mass wind travelling in a divergent jet.

Infrared spectroscopy of jets is as yet in its infancy. Although searches for strong emission in molecular hydrogen ($2.12 \mu\text{m}$) in the highly collimated jets of HH34, M78 and HH1/HH2 have been unsuccessful, recent infrared array observations of HH46/47 clearly show a faint, well collimated red-shifted jet (Zealey, unpublished). Velocity profiles observed in the broad HH7-11 jet show extended H_2 plateau emission 200 km s^{-1} wide (Zinnecker *et al.* 1989). Such low excitation emission exhibiting large velocity dispersions may arise at the edge of the flow from entrained, shocked material or by reflection from dust.

Recent observations of [FeII] emission at $1.67 \mu\text{m}$ in the HH34 jet and several other HH objects indicate that excitation conditions similar to those producing the [SII] visible emission occur in the jet (Stapelfeldt *et al.* 1991).

Dynamics of jets (proper motion and radial velocity): In all jets, large radial velocities of the order of $100\text{--}200 \text{ km s}^{-1}$ directed away from the central stars are observed. Relatively high velocity dispersions of up to 100 km s^{-1} are commonly observed. Jets terminating in bright HH objects show evidence for deceleration at their ends, supporting the idea that these are indeed the working surfaces of the outflows.

Although a considerable amount of data on the proper motion of HH objects associated with the working surfaces of the jets is available, little comparable information is available for the jets themselves. Neckel and Staude (1987) have found transverse velocities of 190 km s^{-1} in the knots in the L1551 jet.

With the exception of R Mon the dynamical ages, based on radial velocity and the extent of the jet, range from a hundred to a few thousand years (Mundt *et al.* 1987). This is on average a factor of ten less than the estimated age of the optical outflow phase.

Theoretical models of jets: The discovery of jets in objects as distinct as pre-main-sequence sources, evolved stars and extragalactic objects has led to a search for a common, universal mechanism to explain so widespread a phenomenon. The main areas requiring explanation are those of the wind generation mechanism, the jet collimation mechanism and the jet propagation mechanism. Direct observation of the jet forming regions close to the stellar surface is difficult, hence the question of the formation mechanism is at present largely unanswered.

It has been proposed by Konigl (1982) and others that the energetic outflows associated with young stellar objects are due in some way to massive, circumstellar disks. Stellar mass loss from FU Orionis stars and other young stellar objects may be spherically symmetric but collimated close to the star due to the formation of Laval nozzles. Some winds might possibly be intrinsically bipolar and collimated at the source. Subsequent collimation by a dense circumstellar disk may well result in a highly collimated flow.

Once collimated the jets may develop instabilities and internal shock structures visible as strings of emission knots. The knots in the highly collimated, astrophysical jets appear similar to the luminous shock cones seen in the exhausts of jet engines. This has led to an explanation of the knots in terms of internal shock structures or 'Mach disks' in the flow (Norman *et al.* 1984; Wilson and Falle 1985) (see Fig. 7 below). Such internal shocks may be excited as the jet over-expands on leaving the 'nozzle', and then is reconfined. The process may be repeated until the jet expands freely and ceases to be visible. The outflowing material thus encounters a series of stationary shocks or Mach disks as it moves down the jet axis. The proper motions and radial velocities observed in jets disagree with the stationary shock structures expected from a steady wind (Herbig and Jones 1983; Jones and Walker 1985). They might be matched by an unsteady or periodic outflow.

An alternative explanation may lie in Kelvin-Helmholtz instabilities in the flow (Buhrke *et al.* 1988). Such instabilities occur when two fluids move across each other while in pressure equilibrium. Where the jet is denser than its surroundings, surface waves at the interface between the jet and the surrounding medium narrow the jet (Norman *et al.* 1984). The formation of internal shock waves produces regularly spaced emission, travelling at velocities close to that of the jet.

In the case of a diffuse jet, in which the jet density is less than the surrounding density, it is suggested that the head is embedded in a thick cocoon of backflowing gas (Norman *et al.* 1984). Perturbations in this cocoon or instabilities at its surface may excite shock waves in the jet. These are predicted to be less regular than those for a dense jet.

(3c) *Free Expansion Zone*

As the outflow moves down the density gradient it eventually encounters a region where it is over-pressure and expands freely into a lower density region. In the absence of internal shocks the jet ceases to be visible. A large diameter wind cavity formed by backflowing gas from the working surface of the jet, or by a wind driven from the disk itself, may also develop (Moneti *et al.* 1988). Material in this slow wind can appear as limb brightened molecular emission, recently observed in L1551 (Lizano *et al.* 1988; Rainey *et al.* 1987).

(3d) *The Working Surface*

Morphology of the working surface: Two classes of structure are observed at the tips of outflows. In the first the outflow terminates in a diffuse archlike structure, which often contains small emission knots (HH7, HH1, HH34). In the

second the smooth arc structure is replaced by a looser cluster of emission knots (HH2, HH24, HH54A, HH19).

HH1 appears to be a classical example of an arcuate working surface. Visible [SII] emission caps the tip of the outflow and has the shape of a typical radiative bow shock (Raga *et al.* 1988). Both the visible and H₂ emission exhibit an asymmetry about the axis of the outflow, reflecting density variations in the ambient medium into which the flow expands. The H₂ emission peaks towards the eastern wing of the working surface, and is not present at the apex of the flow (Fig. 6).

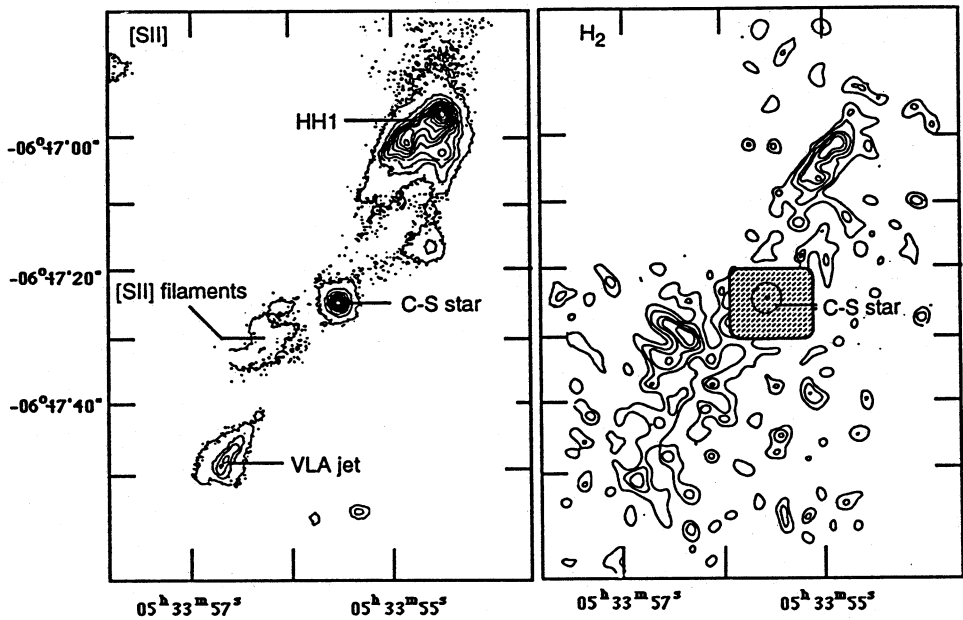


Fig. 6. CCD (SII) and 2 μ m images of HH1 (3.8 m AAT and 3.5 m Calar Alto).

The cluster of emission nebulosities associated with HH2 could result from either several cloudlets moving with the hollow impacting the ambient medium, the interaction of the outflow with a very clumpy ambient medium, or instabilities in the working surface (Raga and Bohm 1987).

In HH54, like HH1 and HH2, the northern tip of the flow appears to be a fragmented cluster of emission nebulosities, while the southern flow ends in a single cusp.

Spectroscopy of the working surface: The observed emission line ratios from neutral atoms [OI], [CI], NI and low excitation ions [SII], [CaII] are typical of those expected in cooling regions behind shock waves (Schwartz 1978). Variations in these line ratios are interpreted as being due to different excitation conditions and hence shock velocities. In the 1980s it became clear that emission from different ionic species could be produced in different parts of non-planar shocks (Hartigan *et al.* 1987). Considerable work has since been expended by Hartigan

(1989), Solf (1989) and Raga (1989) in interpreting the appearance of long slit spectra in terms of bow shock morphology.

In the infrared, H_2 line profiles allow us to study the lowest shock velocities present in wings of bow shocks (Doyon and Nadeau 1988; Zinnecker *et al.* 1989). The strength of these emissions have made it clear that proper modelling of shock conditions and emission line ratios must incorporate the contribution H_2 makes to post-shock cooling.

Theory of the working surface: Several models have been proposed to explain HH objects. These have involved shock excitation associated with cloudlets accelerating in a supersonic outflow (Schwartz 1978) or associated with jets and high velocity cloudlets clouds impacting the interstellar medium (Canto 1980; Norman and Silk 1979).

The most successful theory is that of a jet impacting the ISM. At the working surface the outflow is expected to shock and, in turn, be shocked by the ambient medium (Mundt 1985). The collimated flow terminates in a pair of shocks; a shock in which material from the ISM is accelerated (the bow shock) and a shock in which material from the jet is decelerated (Mach disk of jet shock) (see Fig. 7). For a heavy jet, it is expected that material in the outflow will be shocked only weakly, but have a high velocity. Ambient cloud material entering the bow shock at its apex will be highly shocked and rapidly accelerated to the outflow velocity. Molecular material will be dissociated in this region. Cloud material passing through the oblique shock in the wings of the bow shock will be less shocked and less accelerated, allowing molecular material to be excited but not dissociated. Molecular emission is to be expected from the wings of such a bow shock. Comparison of velocity profiles of the infrared H_2 and visible emission lines (Zinnecker *et al.* 1989) support this view.

It has been suggested that the differences in morphology of the terminal HH objects reflect instabilities in the working surfaces and result from the outflow encountering different density gradients. The arcuate nebulosities may imply that the flow is density bounded (Blondin *et al.* 1989). An extreme example of this is to be found in HH24, where the south-eastern blue shifted jet ends in a bright extended HH object as it encounters a dense clump of stationary material. The red shifted jet apparently expands freely to the north-west (Zealey *et al.* 1989).

4. Confusions and Conclusions

We have come a long way in understanding the general mechanism underlying stellar outflows since the early work of Herbig and Haro. The detailed theory is less well understood. Observations from the far ultraviolet to centimetre wavelengths, made with widely different spatial and spectral resolutions, provide the basis for understanding the flows. It is not surprising that it is proving difficult to weld these observations into a detailed coherent model of outflows. Two firm statements relating to observations may be made at this stage:

(1) There is strong evidence for the existence of disks around the driving sources which are probably capable of collimating the outflow. However, it is not yet clear whether other mechanisms play a part in the collimation.

(2) The predominant ultraviolet, visible and infrared emission mechanism involved in the Herbig-Haro phenomenon is shock excitation. In many cases these

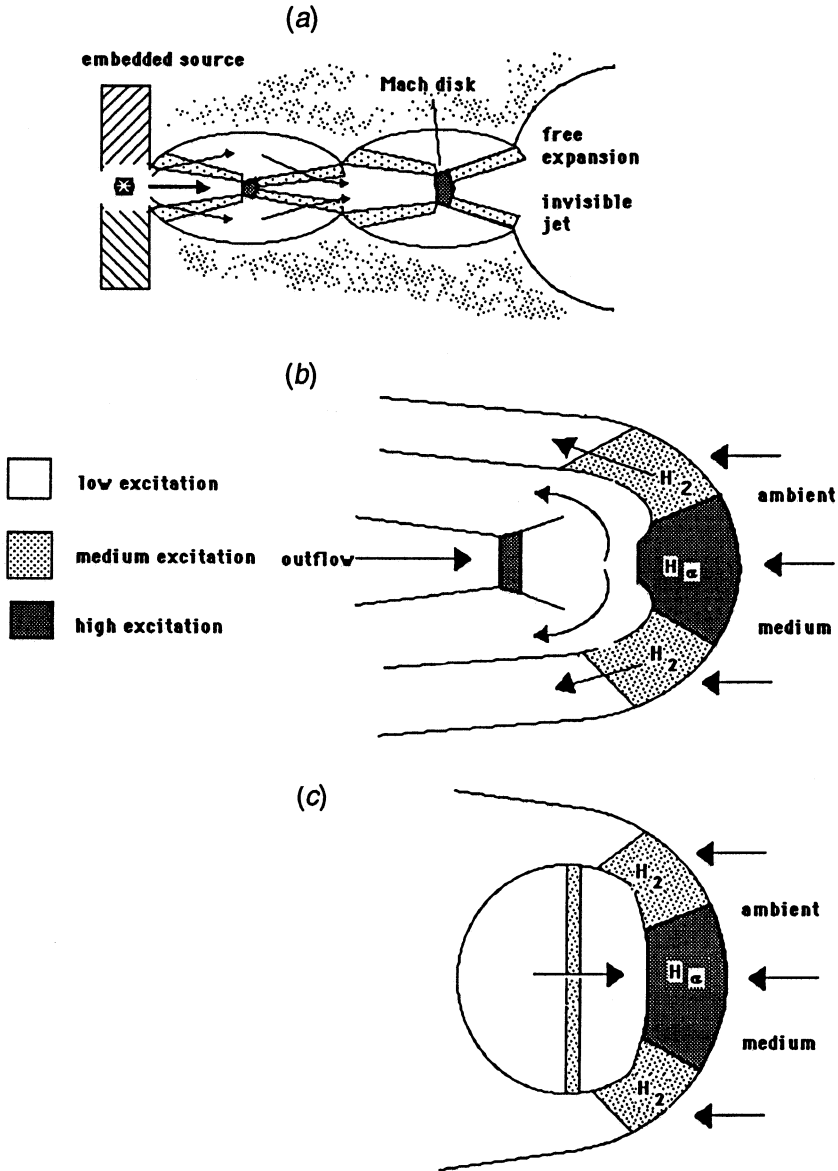


Fig. 7. Diagrams illustrating: (a) the formation of shocks in a Mach disk in a well collimated jet; (b) the formation of shocks in a fast moving clouddlet encountering the ISM; and (c) the formation of shocks in a jet encountering the ISM. The position of cooling regions associated with high and low excitation emission lines are indicated.

shocks are associated with the working surface of the outflow as it encounters the interstellar medium.

Many fundamental questions require a combination of observations beyond the limits of current instrumentation and computer intensive modelling of non-planar

shocks. For these reasons the following questions remain largely unanswered:

- * Do 'molecular outflows' and 'optical bipolar outflows' differ only as a result of the luminosity of the driving source, or are there other fundamental differences?
- * What is the origin of the stellar outflow?
- * What part do outflows play in star formation? Do they represent a significant mechanism for losing angular momentum?
- * How long does the mass loss phase last?
- * How much of the outflow is stellar material? How much entrained ISM?
- * How do the jets remain collimated over large distances?

Acknowledgments

My thanks must go to all the staff at the AAT, UKIRT and ESO who made possible many of the observations presented. Particular acknowledgment is due to B. Reipurth, and R. Mundt for taking frames of HH54 and HH1.

References

- Appenzeller, I. (1989). *Astron. Astrophys. Review* **1**, 291.
- Aspin, C., McCaughrean, M. J., Casali, M. M., and Geballe, T. R. (1992). *Astrophys. J.* (in press).
- Berrilli, F., Ceccarelli, C., Liseau, R., Lorenzetti, D., Saraceno, P., and Spinoglio, L. (1989). *Mon. Not. R. Astron. Soc.* **237**, 1.
- Bieging, J. H., Cohen, M., and Schwartz, P. R. (1986). *Astrophys. J.* **253**, 707.
- Blondin, J. M., Konigl, A., and Fryxell, B. A. (1989). *Astrophys. J. (Lett.)* **357**, L37.
- Brown, A. (1987). *Astrophys. J.* **322**, L31.
- Buhrke, T., Mundt, R., and Ray, T. P. (1988). *Astron. Astrophys.* **200**, 99.
- Canto, J. (1980). *Astron. Astrophys.* **86**, 327.
- Carr, J. S. (1989). *Astrophys. J.* **345**, 522.
- Cohen, M., Jones, B. F., and Herefeld, M. (1987). *Astrophys. J.* **371**, 237.
- Doyon, R., and Nadeau, D. (1988). *Astrophys. J.* **334**, 883.
- Evans, N. J., and Lada, E. A. (1991). Proc. IAU Symp. 147 on Fragmentation of Molecular Clouds and Star Formation (Eds E. Falgarone and G. Dulvert), p. 293 (Kluwer: Dordrecht).
- Hartigan, P. (1989). *Astrophys. J.* **339**, 987.
- Hartigan, P., Raymond, J., and Hartmann, L. (1987). *Astrophys. J.* **316**, 323.
- Herbig, G. H., and Jones, B. J. (1983). *Astron. J.* **88**, 1040.
- Jones, B. F., and Herbig, G. H. (1982). *Astron. J.* **87**, 1223.
- Jones, B. F., and Walker, C. K. (1985). *Astron. J.* **90**, 1320.
- Konigl, A. (1982). *Astrophys. J.* **261**, 115.
- Lightfoot, J. F., and Glencross, W. M. (1986). *Mon. Not. R. Astron. Soc.* **221**, 993.
- Lizano, S., Heiles, C., Rodriguez, L. F., Koo, B. C., Shu, F. H., Hasegawa, T., Hayashi, S., and Mirabel, I. F. (1988). *Astrophys. J.* **328**, 763.
- McCutcheon, W. H., Dewdney, P. E., Purton, C. R., and Sato, T. (1991). *Astron. J.* **101**, 1435.
- McGregor, P. J., Hyland, H. R., and Hillier, D. J. (1988). *Astrophys. J.* **324**, 1071.
- Moneti, A., Forrest, W. J., Pipher, J. L., and Woodward, C. E. (1988). *Astrophys. J.* **327**, 870.
- Mundt, R. (1985). In 'Protostars and Planets II' (Eds D. Black and M. Mathews), p. 414 (University of Arizona Press).
- Mundt, R. (1988). In 'Formation and Evolution of Low Mass Stars' (Eds A. K. Dupree and M. T. V. Lago), p. 257 (Kluwer: Dordrecht).
- Mundt, R., Brugel, E. W., and Buhrke, T. (1987). *Astrophys. J.* **319**, 275.
- Neckel, T., and Staude, H. J. (1987). *Astrophys. J.* **322**, L27.

- Norman, C., and Silk, J. (1979). *Astrophys. J.* **228**, 197.
- Norman, M. L., Smarr, L., and Winkler, K-H. (1984). In 'Numerical Astrophysics' (Eds J. Contrella *et al.*), p. 88 (Jones and Bartlett: Boston).
- Poetzel, R., Mundt, R., and Ray, T. P. (1989). *Astron. Astrophys.* **224**, L13.
- Raga, A. C. (1989). ESO Workshop on Low Mass Star Formation and Pre-main Sequence Objects, No. 33 (Eds B. Reipurth), p. 281 (European Southern Observatory).
- Raga, A. C., and Bohm, K.-H. (1987). *Astrophys. J.* **323**, 193.
- Raga, A. C., Mateo, M., Bohm, K-H., and Solf, J. (1988). *Astron. J.* **95**, 1783.
- Rainey, R., White, G. J., Richardson, K. J., Griffin, M. J., Cronin, N. J., Montiero, T. S., and Hilton, J. (1987). *Astron. Astrophys.* **179**, 237.
- Reipurth, B. (1989). Proc IAU Symp. on Flare Stars in Star Clusters, Associations and the Solar Vicinity, No. 137 (Eds L. V. Mirozoyan *et al.*), p. 229 (Springer: Berlin).
- Reipurth, B. (1991). Physics of star formation and early stellar evolution. ESO preprint.
- Rodriguez, L. F. (1989). Proc. IAU Colloq. on Structure and Dynamics of the Interstellar Medium, No. 120 (Eds G. Tenorio-Tagle *et al.*), p. 197 (Springer: Berlin).
- Scarrott, S. M., Gledhill, T. M., and Warren-Smith, R. F. (1987). *Mon. Not. R. Astron. Soc.* **227**, 1065.
- Schwartz, R. D. (1977). *Astrophys. J. Suppl.* **35**, 161.
- Schwartz, R. D. (1978). *Astrophys. J.* **223**, 884.
- Schwartz, R. D. (1983). *Ann. Rev. Astron. Astrophys.* **21**, 209.
- Schwartz, R. D. (1985). In 'Protostars and Planets II' (Eds D. Black and M. Mathews), p. 405 (University of Arizona Press).
- Solf, J. (1989). ESO Workshop on Low Mass Star Formation and Pre-main Sequence Objects, No. 33 (Ed. B. Reipurth), p. 339 (European Southern Observatory).
- Stapelheldt, K. R., Beichman, C. A., Hester, J. J., Scoville, N. Z., and Gautier, T. N. (1991). *Astrophys. J.* **371**, 226.
- Suters, M. G., and Zealey, W. J. (1991). *Proc. Astron. Soc. Aust.* **9**, 140.
- Wilson, M. J., and Falle, S. A. G. (1985). *Mon. Not. R. Astron. Soc.* **216**, 971.
- Zealey, W. J., Mundt, R., Ray, T. P., Sandell, G., Geballe, T., Taylor, K. N. R., Williams, P. M., and Zinnecker, H. (1989). *Proc. Astron. Soc. Aust.* **8**, 62.
- Zealey, W. J., Williams, P. M., Sandell, G., Taylor, K. N. R., and Ray, T. P. (1992). *Astron. Astrophys.* (in press).
- Zinnecker, H., Mundt, R., Geballe, T. R., and Zealey, W. J. (1980). *Astrophys. J.* **342**, 337.

